

Supramolecular Strands

Meter-Long and Robust Supramolecular Strands Encapsulated in Hydrogel Jackets**

Daisuke Kiriya, Masato Ikeda, Hiroaki Onoe, Masahiro Takinoue, Harunobu Komatsu, Yuto Shimoyama, Itaru Hamachi, and Shoji Takeuchi*

The self-assembly of organic molecules, termed supramolecular assembly, has been reported extensively from nanosized molecular clusters to microscale assemblies.^[1–9] Increasing attention has recently focused on macroscopic supramolecular assembly within the millimeter to centimeter range.^[10–13] Assemblies on this scale display both molecular and macroscopic benefits, such as structural flexibility and shape adjustability. These structures are usually constructed from specific oligomers with multiple interaction sites for shape retention. However, typical supramolecular assemblies such as phospholipid structures are constructed with a limited number of interactions such as hydrogen bonding and/or π - π and van der Waals interactions between molecules. These weak interactions inhibit the construction of macroscopic assemblies.^[8,14] For the fabrication of macroscopic supramolecular assemblies even in these molecules, two factors are required: 1) the dense and oriented packing of molecular assemblies to enhance molecular interactions^[15] and 2) robust support for shape retention of supramolecular assemblies. With these two factors, we developed a simple method for fabrication of densely aligned supramolecular nanofibers jacketed in a robust hydrogel on the meter scale, using microfluidic techniques.

Figure 1 shows the supramolecular assemblies targeted in this research. The supramolecular monomer used here is a lipid-type molecule (monomer **1**)^[16] that forms nanofibers.

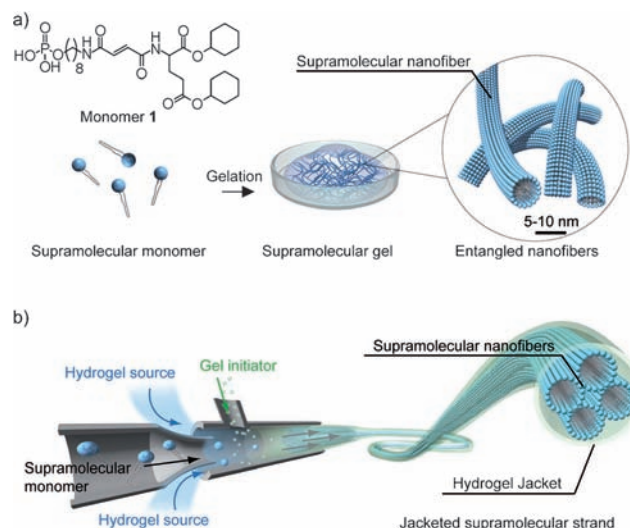


Figure 1. Supramolecular gels fabricated both in bulk and in a microfluidic channel. a) Bulk sample of the supramolecular gel. Monomers are assembled to form supramolecular nanofibers that are entangled with each other to form a supramolecular gel. The chemical structure of the phospholipid-type supramolecular monomer (**1**) used herein is included. b) A process for producing jacketed supramolecular strands fabricated in a coaxial flow microfluidic device. The coaxial laminar flows of the supramolecular monomer and the hydrogel polymer source solutions are enclosed by a gel initiator solution to form a coaxial gel cable (jacketed supramolecular strand). The supramolecular nanofibers are aligned in the hydrogel jacket.

[*] Dr. D. Kiriya, Dr. H. Onoe, Dr. M. Takinoue, Y. Shimoyama, Prof. S. Takeuchi

Institute of Industrial Science, The University of Tokyo
 4-6-1 Komaba, Meguro-ku, Tokyo 153-8505 (Japan)
 E-mail: takeuchi@iis.u-tokyo.ac.jp

Dr. D. Kiriya, Dr. M. Ikeda, Prof. I. Hamachi, Prof. S. Takeuchi
 Japan Science and Technology Agency (JST), CREST
 5 Sanbancho, Chiyoda-ku, Tokyo 102-0075 (Japan)

Dr. D. Kiriya, Dr. H. Onoe, Prof. S. Takeuchi
 ERATO Takeuchi Biohybrid Innovation Project, JST
 Komaba Open Laboratory (KOL) Room M202
 4-6-1, Komaba, Meguro-ku, Tokyo, 153-8904 (Japan)

Dr. M. Ikeda, Dr. H. Komatsu, Prof. I. Hamachi
 Department of Synthetic Chemistry and Biological Chemistry
 Graduate School of Engineering, Kyoto University
 Katsura, Nishikyo-ku, Kyoto 615-8510 (Japan)

[**] This work was supported by the JST (Japan Science and Technology Agency). We thank N. Saito, I. Obataya, and T. Sugitate (JPK Instruments Co.) for the support of AFM measurement, K. Kuribayashi (The University of Tokyo) for help to take microscope images and the pictures of supramolecular strands with 1 m length.



Supporting information for this article is available on the WWW under <http://dx.doi.org/10.1002/anie.201104043>.

The nanofibers are three-dimensionally entangled, forming fragile macroscopic gels in bulk (see Figure 1a and Movie S1 in the Supporting Information).^[17] To improve the molecular interactions, we attempted to fabricate the supramolecular assemblies in a microfluidic channel. The supramolecular assemblies should align because of shear stress provided by the laminar flow in the channel (Figure 1b). Similar hydrodynamic orientations have already been observed in the case of inorganic rods,^[18] DNA strands,^[19] carbon nanotubes,^[20] and organic polymers.^[21] Furthermore, we encapsulated the supramolecular nanofibers (strands) in a robust hydrogel matrix (hydrogel jacket) to form a long core-shell-type gel cable (jacketed supramolecular strand) using a co-axial laminar flow.

We used a microfluidic device to create a jacketed supramolecular strand (see Figure 2a and Figure S1 in the Supporting Information). With this device, the supramolecular strand was jacketed by a calcium alginate gel, which expected to enhance the stability and robustness of the

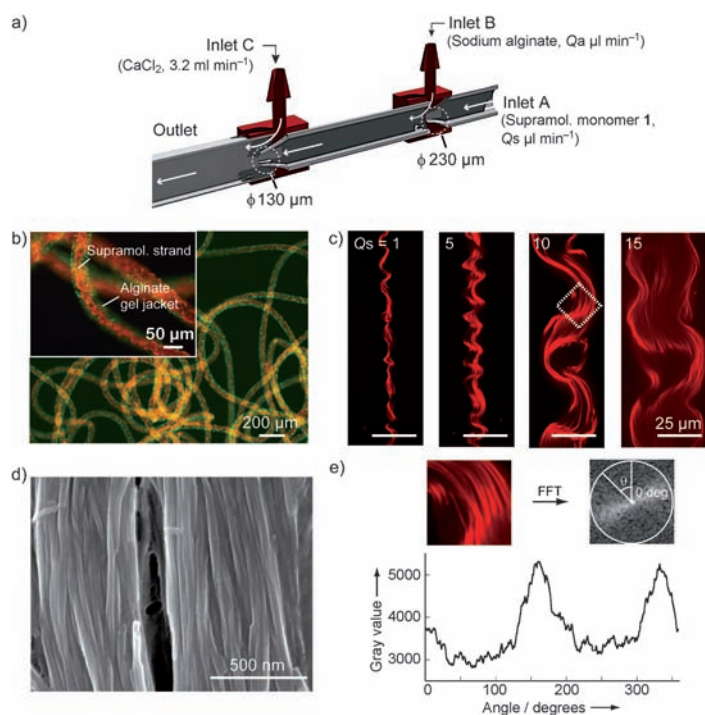


Figure 2. Jacketed supramolecular strand fabrication. a) The microfluidic device used herein. Sample solutions were introduced through three inlets (A, B, and C), and jacketed supramolecular strands were obtained from the outlet. The monomer **1** ($Q_s \mu\text{L min}^{-1}$), sodium alginate ($Q_a \mu\text{L min}^{-1}$), and CaCl_2 (3.2 mL min^{-1}) solutions were introduced into Inlets A, B, and C, respectively. The total volume flow rate was $Q_s + Q_a = 20 \mu\text{L min}^{-1}$. b) Fluorescence microscopy image of the jacketed supramolecular strands ($Q_s = 10 \mu\text{L min}^{-1}$) visualized by green-fluorescent nanobeads (alginate gel jacket) and R18 dye (supramolecular strands). c) CLSM images of the supramolecular nanofibers in jacketed supramolecular strands fabricated with variable volume flow rates. The supramolecular nanofibers were visualized using the R18 dye. d) SEM image of the aligned supramolecular nanofibers after the alginate gel jacket was removed. e) 2D FFT analysis calculated for the selected area shown in Figure 2c ($Q_s = 10 \mu\text{L min}^{-1}$) and a plot of the corresponding summed pixel intensity from the FFT image along a straight line radiating at the angle. This plot indicates that the supramolecular nanofibers were orientated perpendicular to 160° and 340° .

structure.^[22] The supramolecular monomer fluid (solution of 0.1 wt% monomer **1**) and sheath fluid (1.5 wt% sodium alginate solution with lipid dyes and green-fluorescent nanobeads) were introduced into Inlets A and B, respectively, and these sample flows were surrounded by 20 mM CaCl_2 solution introduced through Inlet C (Figure 2a). The total volume flow rate of monomer **1**, Q_s ($\mu\text{L min}^{-1}$), and alginate, Q_a ($\mu\text{L min}^{-1}$), was $20 \mu\text{L min}^{-1}$. Both samples became gels after combining with the CaCl_2 solution in the channel. The supramolecular strand and alginate gel jacket were visualized using lipid dyes and fluorescent nanobeads, respectively (see the Supporting Information).

The morphologies of the obtained strands were examined. Fluorescence microscopy imaging revealed that a jacketed supramolecular strand of approximately $50 \mu\text{m}$ in diameter was successfully formed (see Figure 2b and Figure S2 and Movies S2 and S3 in the Supporting Information). Confocal laser scanning microscopy (CLSM) imaging indicated that the supramolecular fibrous assemblies are aligned along one

direction at the macroscopic scale (see Figure 2c and Figure S3 in the Supporting Information). Scanning electron microscopy (SEM) imaging revealed a detailed structure in which supramolecular nanofibers with diameters of approximately 40 nm were aligned along the direction of the jacketed supramolecular strands (see Figure 2d and Figure S4 in the Supporting Information). In contrast, the supramolecular nanofibers in the bulk supramolecular gel showed a three-dimensional entangled network (see Figure S3 in the Supporting Information).

The orientation of the supramolecular nanofibers was investigated by fast Fourier transform (FFT) analysis. FFT was used to characterize the square region (64×64 pixels) indicated in Figure 2c ($Q_s = 10 \mu\text{L min}^{-1}$). The resultant FFT output image contained grayscale pixels distributed in an elliptical pattern that reflected the degree of supramolecular nanofiber orientation (see Figure 2e and Figure S5 in the Supporting Information). A plot of the corresponding summed pixel intensity from the FFT image indicated that the supramolecular nanofibers were strongly orientated perpendicular to the peaks in the plot (160° and 340°). We evaluated the orientation value (S) of the nanofibers, which tends to 0 for those that are perfectly oriented along one axis and to 1 for an isotropic distribution (S is defined in the Supporting Information).^[23,24] The S value of the supramolecular nanofibers in the jacketed supramolecular strand was calculated to be 0.70, which is smaller than that for the supramolecular nanofibers within the bulk gel ($S = 0.95$, see Table S1 in the Supporting Information). This value includes the effect of a wave-like structure. However, the S value of the jacketed supramolecular strands is obviously smaller than that of the bulk. We found that the encapsulated supramolecular structures grew primarily in one direction and were aligned with the laminar flow in the microfluidic channel. Additionally, aligned structures can be observed in the supramolecular strands without the alginate gel jacket ($Q_s = 20 \mu\text{L min}^{-1}$, see Figure S3 in the Supporting Information). Therefore, the microfluidic fabrication process is a key factor for obtaining aligned supramolecular structures. However, the supramolecular strand without the alginate gel jacket was extremely fragile. The sample could not be picked up from a collection flask.

The jacketed supramolecular strands were easy to handle and could be used to form macroscopic patterns and arrangements. First, the robust hydrogel jackets allow us to manually handle differently colored supramolecular strands to arrange them on glass (Figure 3a). Vertically and horizontally arranged supramolecular strands were visualized by R18 dyes and fluorescein isothiocyanate (FITC) lipid,^[25] respectively. The patterned jacketed supramolecular strands are useful for the detection and quantification of temporal changes around the strands. Using the FITC moiety embedded in the strand as a pH indicator,^[26] we monitored fluorescence changes associated with a pH change. The green fluorescence of the supramolecular strands is dramati-

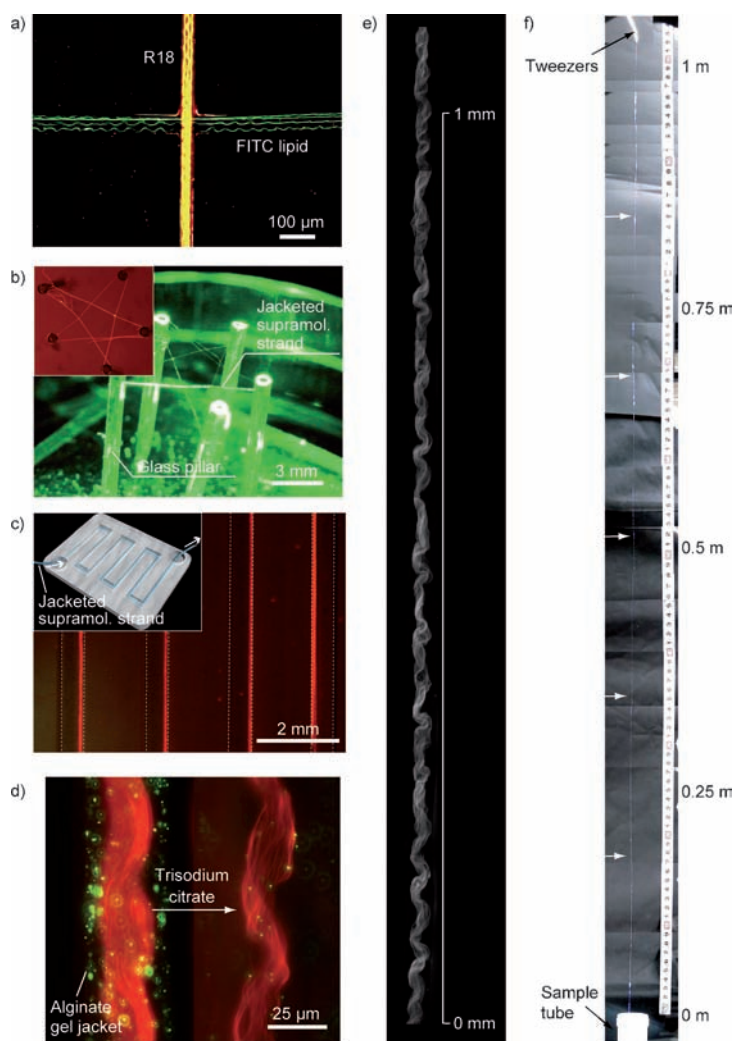


Figure 3. Handling of the jacketed supramolecular strands. a) Fluorescence microscopy image showing the arrangement of differently colored jacketed supramolecular strands on a glass substrate. The vertically and horizontally arranged supramolecular strands were visualized by R18 dyes and FITC lipid, respectively. b) Photograph of a single jacketed supramolecular strand bridging five glass pillars to form a star shape in air. Inset) Overhead view of the star shape, as observed by fluorescence microscopy. The supramolecular strand was visualized by the R18 dye. c) Fluorescence microscopy image of a jacketed supramolecular strand arranged in a microfluidic channel. The supramolecular strand was visualized by the R18 dye. Inset) Image of the arrangement. d) Images before and after the alginate gel jacket was removed (visualized by green-fluorescent nanobeads) by the introduction of sodium citrate into the microfluidic channel. e) CLSM image of the macroscopically aligned supramolecular nanofibers in the microfluidic channel. f) Sequential images of a meter-long supramolecular strand pulled from a sample tube using a pair of tweezers. All jacketed supramolecular strands were prepared with $Q_s = 10 \mu\text{L min}^{-1}$.

ically reduced by changing the environmental pH from 8.6 to 5.0 (see Figure S6 in the Supporting Information), which indicates that the jacketed supramolecular strands can be functionalized as a fluorescent sensor using the accompanying stimuli-responsive lipid in the strand. Second, we successfully constructed a free-standing pattern (star shape) of the supramolecular assembly by bridging a jacketed supramolecular strand between glass pillars (see Figure 3 b and Figure S7

in the Supporting Information). This demonstration indicates the sufficiently high mechanical strength of the jacketed supramolecular strands. We also attempted to arrange and immobilize the jacketed supramolecular strands into desired positions using a microfluidic channel (Figure 3 c). After immobilization of the jacketed supramolecular strands, the alginate gel jacket can be removed by introducing a sodium citrate solution into the microfluidic channel.^[27] As a result, the structures of the aligned supramolecular nanofibers were sustained in the channel in the absence of the alginate gel jacket (Figure 3 d). These applications show that the method allows for the spatial arrangement of weak supramolecular assemblies into desired positions.

The detailed macroscopic structures of the supramolecular strands can be analyzed according to their handleability. Figure 3 e shows sequential CLSM images of macroscopic supramolecular strands immobilized in the microfluidic channel. Macroscopic ordering of the nanofibers on a scale of several millimeters was observed, which is attributed to the sample immobilization in the microfluidic channel (see Figure 3 e and Figure S8 in the Supporting Information). The overall length of the supramolecular strands could be easily adjusted by changing the sample injection time during the strand formation process. Figure 3 f shows a jacketed supramolecular strand over 1 m in length that was pulled from a sample tube using a pair of tweezers (see Movie S4 in the Supporting Information). Surprisingly, the shape of the jacketed supramolecular strand was retained through this process. This shape retention is due to the support of the alginate gel jacket.

We envisioned the practical application of macroscopically aligned supramolecular nanofibers in jacketed supramolecular strands as a template for the polymerization of insoluble conductive polymers (Figure 4 a). Because the supramolecular nanofibers are constructed through van der Waals interactions and hydrogen bonds of lipid tail moieties and the complexation between phosphate moieties and calcium ions, it is expected that guest molecules can be concentrated along the supramolecular nanofibers through multiple interactions, including hydrogen-bond, Coulomb, and van der Waals interactions. We carried out template synthesis of poly(aniline) (PANI) using the jacketed supramolecular strands by immersing them in an aqueous solution containing 48 mM anilinium chloride. The supramolecular nanofibers were expected to absorb the anilinium cations. The colorless strands obtained were then immersed into a 1 M acetic acid solution (pH 2.3) of 0.15 mM ammonium peroxydisulfate (APS) for oxidative polymerization of the PANI. As a result of this procedure, a green cable was obtained (Figure 4 b). This color is well-known as an emeraldine salt of PANI.^[28] The cables showed sufficient mechanical strength to be handled by a pair of tweezers, similar to the strands before the template synthesis (Figure 4 c). Under bright field mi-

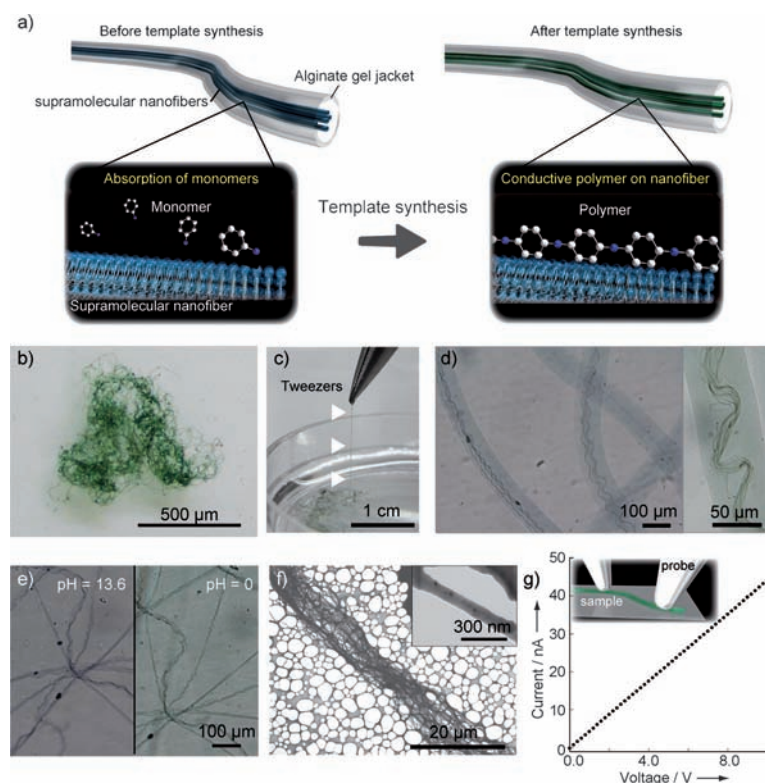


Figure 4. Template synthesis of PANI using jacketed supramolecular nanofibers. a) Procedure for the synthesis of PANI nanofibers. b) A green cable obtained after the reaction protocol for the preparation of PANI and c) a demonstration of the handleability of the green cable. d) Bright field microscopy image of the green cable. The green strands are encapsulated in the alginate gel jacket. e) Bright field microscopy images of the PANI nanofibers after immersion in EDTA solution (pH 13.6) to remove the alginate gel jacket (left) and further immersion in 1 M HCl (pH 0, right). f) STEM images of the PANI nanofibers on a grid, showing that the fibrous structures are ordered. Inset) An enlarged image of a PANI nanofiber with a diameter of approximately 60 nm. g) Current–voltage plot of PANI nanofibers, measured using probes. Inset) Image of the measurement.

scopy, aligned dark green fibers (dark green strands) were clearly observed inside the green cable (Figure 4d). Ethylenediaminetetraacetic acid (EDTA, 0.25 M, pH 13.6) was used to remove the supramolecular template and the alginate gel jacket.^[16,29] We isolated a dark blue strand without the alginate gel jacket (see Figure 4e and Movie S5 in the Supporting Information) that showed a different color than the as-synthesized dark green strand; this was achieved by a redox reaction of PANI through a change of pH.^[28] In fact, the blue strands showed a pH-dependent color change. Immersion in 1 M HCl solution (pH 0) induced the reverse redox reaction to produce a green strand (Figure 4e). Emphasis is placed on these dark green/blue strands that show a morphology similar to that of the template supramolecular strand in Figure 2c. This result indicates that the supramolecular strands can act as a template for the synthesis of PANI.

To identify the green strand, we carried out the following experiments. In the Fourier transform infrared (FT-IR) spectrum of the obtained green strands, peaks were observed at approximately 1135, 1235, 1300, 1485, and 1570 cm^{-1} , which are identical to those of the emeraldine salt form of PANI (see

Figure S9a,b in the Supporting Information).^[30] Scanning transmission electron microscope (STEM) images showed that the aligned nanofibers had a diameter of approximately 60 nm (see Figure 4f and Figure S9c,d in the Supporting Information). These results further support our view that aligned PANI nanofibers formed during template synthesis on the aligned supramolecular nanofibers in the jacketed supramolecular strands. Recently, several research groups have attempted to synthesize PANI nanofibers using inorganic porous materials^[31] or tiny soft templates, such as lipids or supramolecular structures.^[14,32] However, the PANI nanofibers isolated in previous studies showed micrometer scale fragments that were strongly aggregated. In contrast, our template synthesis of aligned supramolecular nanofibers in jacketed supramolecular strands allows us to maintain the morphology of the nanofibers without aggregation. Therefore, our approach enables the construction of morphologically controlled PANI nanofibers that are easy to handle because of the hydrogel jacket. Finally, we measured the conductivity of the PANI nanofibers, as shown in Figure 4g. The conductivity of the PANI nanofibers after removing the alginate gel jacket was estimated to be 0.75 S m^{-1} (see Figure 4g and Figure S9e,f in the Supporting Information). The value is on the order of several tens of nanoamperes, which is sufficient for use as a sensor material. Our strategy of template synthesis using jacketed supramolecular strands would be useful for synthesizing handleable aligned organic conductive nanofibers.

We have shown a method involving microfluidic techniques for the fabrication of meter-scale aligned supramolecular nanofibers encapsulated in a hydrogel jacket. The jacketed supramolecular nanofibers can be used as templates not only for conductive polymers such as PANI, but also for other organic molecules, biochemical molecules such as proteins, nanoparticles, and metals for generating large oriented materials that are similar to those found in nature. We believe that this approach is a major advance in the realization of large-scale supramolecular structures with defined shapes, including one-dimensional coils, two-dimensional fabric sheets, and three-dimensional constructs.

Received: June 13, 2011

Revised: October 21, 2011

Published online: November 15, 2011

Keywords: hydrogels · microfluidics · self-assembly · supramolecular chemistry · template synthesis

[1] J.-M. Lehn, *Supramolecular Chemistry: Concepts and Perspectives*, VCH, Weinheim, 1995.

- [2] A. R. Hirst, B. Escuder, J. F. Miravet, D. K. Smith, *Angew. Chem.* **2008**, *120*, 8122–8139; *Angew. Chem. Int. Ed.* **2008**, *47*, 8002–8018.
- [3] G. A. Silva, C. Czeisler, K. L. Niece, E. Beniash, D. A. Harrington, J. A. Kessler, S. I. Stupp, *Science* **2004**, *303*, 1352–1355.
- [4] S. G. Zhang, *Nat. Biotechnol.* **2003**, *21*, 1171–1178.
- [5] J. E. Green, J. W. Choi, A. Boukai, Y. Bunimovich, E. Johnston-Halperin, E. Delonno, Y. Luo, B. A. Sheriff, K. Xu, Y. S. Shin, H. Tseng, J. F. Stoddart, J. R. Heth, *Nature* **2007**, *445*, 414–417.
- [6] N. Tuccitto, V. Ferri, M. Cavazzini, S. Quici, G. Zhavnerko, A. Licciardello, M. A. Rampi, *Nat. Mater.* **2009**, *8*, 41–46.
- [7] L. Schmidt-Mende, A. Fechtenkötter, K. Müllen, E. Moons, R. H. Friend, J. D. MacKenzie, *Science* **2001**, *293*, 1119–1122.
- [8] G. M. Whitesides, J. P. Mathias, C. T. Seto, *Science* **1991**, *254*, 1312–1319.
- [9] J.-M. Lehn, *Science* **2002**, *295*, 2400–2403.
- [10] Q. Wang, J. L. Mynar, M. Yoshida, E. Lee, M. Lee, K. Okubo, K. Kinbara, T. Aida, *Nature* **2010**, *463*, 339–343.
- [11] P. Cordier, F. Tournilhac, C. Soulié-Ziakovic, L. Leibler, *Nature* **2008**, *451*, 977–980.
- [12] S. Zhang, M. A. Greenfield, A. Mata, L. C. Palmer, R. Bitton, J. R. Mantei, C. Aparicio, M. O. Cruz, S. I. Stupp, *Nat. Mater.* **2010**, *9*, 594–601.
- [13] D. Yan, Y. Zhou, J. Hou, *Science* **2004**, *303*, 65–67.
- [14] K. Sada, M. Takeuchi, N. Fujita, M. Numata, S. Shinkai, *Chem. Soc. Rev.* **2007**, *36*, 415–435.
- [15] M. J. Buehler, *Nat. Nanotechnol.* **2010**, *5*, 172–174.
- [16] H. Komatsu, S. Matsumoto, S. Tamaru, K. Kaneko, M. Ikeda, I. Hamachi, *J. Am. Chem. Soc.* **2009**, *131*, 5580–5585.
- [17] M. Ikeda, Y. Shimizu, S. Matsumoto, H. Komatsu, S. Tamaru, T. Takigawa, I. Hamachi, *Macromol. Biosci.* **2008**, *8*, 1019–1025.
- [18] Y. Huang, X. Duan, Q. Wei, C. M. Lieber, *Science* **2001**, *291*, 630–633.
- [19] K. Yamashita, Y. Yamaguchi, M. Miyazaki, H. Nakamura, H. Shimizu, H. Maeda, *Chem. Lett.* **2004**, *33*, 628–629.
- [20] V. A. Davis, A. N. G. Parra-Vasquez, M. J. Green, P. K. Rai, N. Behabtu, V. Prieto, R. D. Booker, J. Schmidt, E. Kesselman, W. Zhou, H. Fan, W. W. Adams, R. H. Hauge, J. E. Fischer, Y. Cohen, Y. Talmon, R. E. Smalley, M. Pasquali, *Nat. Nanotechnol.* **2009**, *4*, 830–834.
- [21] N. Mahajan, J. Fang, *Langmuir* **2005**, *21*, 3153–3157.
- [22] a) C. K. Kuo, P. X. Ma, *Biomaterials* **2001**, *22*, 511–521; b) M. Kobašljija, D. T. McQuade, *Biomacromolecules* **2006**, *7*, 2357–2361.
- [23] C. Ayres, G. L. Bowlin, S. C. Henderson, L. Taylor, J. Shultz, J. Alexander, T. A. Telemeco, D. G. Simpson, *Biomaterials* **2006**, *27*, 5524–5534.
- [24] L. Sardone, V. Palermo, E. Devaux, D. Credgington, M. Loos, G. Marletta, F. Cacialli, J. Esch, P. Samori, *Adv. Mater.* **2006**, *18*, 1276–1280.
- [25] S. Tamaru, M. Ikeda, Y. Shimidzu, S. Matsumoto, S. Takeuchi, I. Hamachi, *Nat. Commun.* **2010**, DOI: 10.1038/ncomms1018.
- [26] R. Aoun, A. Yassin, M. E. Jamal, A. Kanj, J. Rault-Berthelot, C. Poriel, *Synth. Met.* **2008**, *158*, 790–795.
- [27] X.-W. Shi, C.-Y. Tsao, X. Yang, Y. Liu, P. Dykstra, G. W. Rubloff, R. Ghodssi, W. E. Bentley, G. F. Payne, *Adv. Funct. Mater.* **2009**, *19*, 2074–2080.
- [28] J. Huang, S. Virji, B. H. Weiller, R. B. Kaner, *J. Am. Chem. Soc.* **2003**, *125*, 314–315.
- [29] T. Braschler, R. Johann, M. Heule, L. Metref, P. Renaud, *Lab Chip* **2005**, *5*, 553–559.
- [30] Z. Wei, L. Zhang, M. Yu, Y. Yang, M. Wan, *Adv. Mater.* **2003**, *15*, 1382–1385.
- [31] C.-G. Wu, T. Bein, *Science* **1994**, *264*, 1757–1759.
- [32] L. Pan, H. Qiu, C. Dou, Y. Li, L. Pu, J. Xu, Y. Shi, *Int. J. Mol. Sci.* **2010**, *11*, 2636–2657.